THE JOURNAL OF BIOLOGICAL CHEMISTRY VOL. 283, NO. 13, pp. 8229–8236, March 28, 2008

Niemann-Pick Type C1 I1061T Mutant Encodes a Functional Protein That Is Selected for Endoplasmic Reticulum-associated Degradation Due to Protein Misfolding*

Received for publication, October 22, 2007, and in revised form, January 23, 2008 Published, JBC Papers in Press, January 23, 2008, DOI 10.1074/jbc.M708735200

Mark E. Gelsthorpe[‡1], Nikola Baumann[‡], Elizabeth Millard[‡], Sarah E. Gale[‡], S. Joshua Langmade[‡], Jean E. Schaffer[‡§], and Daniel S. Ory[‡¶2]

From the [‡]Center for Cardiovascular Research, Departments of Internal Medicine, [§]Molecular Biology and Pharmacology, and [¶]Cell Biology and Physiology, Washington University School of Medicine, St. Louis, Missouri 63110

Over 200 disease-causing mutations have been identified in the *NPC1* gene. The most prevalent mutation, *NPC1*^{I1061T}, is predicted to lie within the cysteine-rich luminal domain and is associated with the classic juvenile-onset phenotype of Niemann-Pick type C disease. To gain insight into the molecular mechanism by which the *NPC1*^{I1061T} mutation causes disease, we examined expression of the mutant protein in human fibroblasts homozygous for the *NPC1*^{I1061T} mutation. Despite similar *NPC1* mRNA levels between wild type and *NPC1*^{I1061T} fibroblasts, NPC1 protein levels are decreased by 85% in *NPC1*^{I1061T} cells. Metabolic labeling studies demonstrate that unlike wild type protein, which undergoes a glycosylation pattern shift from Endo H-sensitive to Endo H-resistant species, NPC1^{I1061T} protein remains almost exclusively Endo H-sensitive and exhibits a reduced half-life ($t_{½}$ 6.5 h) *versus* wild type Endo H-resistant species ($t_{½}$ 42 h). Treatment with chemical chaperones, growth at permissive temperature, or inhibition of proteasomal degradation increases NPC1^{I1061T} protein levels, indicating that the mutant protein is likely targeted for endoplasmic reticulum-associated degradation (ERAD) due to protein misfolding. Overexpression of NPC1^{I1061T} in *NPC1*-deficient cells results in late endosomal localization of the mutant protein and complementation of the *NPC* mutant phenotype, likely due to a small proportion of the nascent NPC1^{I1061T} protein that is able to fold correctly and escape the endoplasmic reticulum quality control checkpoints. Our findings provide the first description of an endoplasmic reticulum trafficking defect as a mechanism for human NPC disease, shedding light on the mechanism by which the *NPC1*^{I1061T} mutation causes disease and suggesting novel approaches to treat NPC disease caused by the *NPC1*^{I1061T} mutation.

Niemann-Pick type C (NPC)[3] disease is a fatal neurodegenerative disease characterized by neuronal lipid storage and progressive Purkinje cell loss in the cerebellum. Mutations in the *NPC1* gene are responsible for ~95% of human NPC disease (1). The human *NPC1* gene encodes a 1278-amino acid polytopic protein containing 13 transmembrane domains, including a pentahelical domain that is evolutionarily and functionally related to sterol-sensing domains found in five other polytopic proteins involved in sterol interactions or sterol metabolism (2, 3). The NPC1 sterol-sensing domain shares ~30% identity with the sterol-sensing domains of 3-hydroxymethylglutaryl-CoA reductase, sterol regulatory element-binding protein cleavage-activating protein (SCAP), NPC1-L1 and Patched (4). A carboxyl-terminal dileucine motif targets NPC1 to the endocytic pathway, where it localizes to a late endosomal compartment that is LAMP-2-positive, Rab7-positive, and cation-independent mannose-6-P receptor-negative (5–7).

The NPC1 protein is a key participant in intracellular sterol trafficking. Cells harboring inactivating mutations in NPC1 exhibit marked impairment of low-density lipoprotein (LDL) cholesterol esterification and mobilization of newly hydrolyzed LDL cholesterol to the plasma membrane (8–10). As a result of these trafficking defects, *NPC1* mutant cells demonstrate lysosomal sequestration of LDL cholesterol, delayed down-regulation of the LDL receptor and *de novo* cholesterol biosynthesis, and impaired ABCA1-mediated cholesterol efflux (11–14).

Over 200 disease-causing mutations have been identified in the *NPC1* gene (15–17). The most prevalent mutation, *NPC1*^{I1061T}, is predicted to lie within a cysteine-rich luminal domain of the NPC1 protein and represents 15–20% of all disease alleles (4, 15, 18). Human fibroblasts homozygous for the *NPC1*^{I1061T} mutation exhibit markedly impaired LDL-stimulated cholesterol esterification and accumulation of unesterified cholesterol in aberrant lysosomes (15). Previous studies have shown that NPC1^{I1061T} is expressed at lower levels and exhibits altered banding patterns on Western blotting as compared with wild type (WT) protein (19). However, the molecular mechanism through which the *NPC1*^{I1061T} missense mutation results in NPC disease is poorly understood.

In the present study we examine the effect of the *NPC1*^{I1061T} substitution on processing and stability of the NPC1 protein. We provide evidence that the NPC1^{I1061T} protein is synthe-

* The costs of publication of this article were defrayed in part by the payment of page charges. This article must therefore be hereby marked "*advertisement*" in accordance with 18 U.S.C. Section 1734 solely to indicate this fact.

[1] Supported by National Institutes of Health Training Grant 5T32HL007275-29.

[2] Supported by National Institutes of Health Grants HL04482 and HL67773 and the Ara Parseghian Medical Research Foundation. To whom correspondence should be addressed: Box 8086, 660 S. Euclid Ave., St. Louis, MO 63110. Tel.: 314-362-8737; Fax: 314-362-0186; E-mail: dory@wustl.edu.

[3] The abbreviations used are: NPC1, Niemann-Pick type C1; CFTR, cystic fibrosis transmembrane regulator; CHO, Chinese hamster ovary; GFP, green fluorescent protein; Endo H, Endoglycosidase H; ER, endoplasmic reticulum; ERAD, ER-associated degradation; IP, immunoprecipitation; LDL, low density lipoprotein; WT, wild type; PBA, 4-phenylbutyric acid.

sized but fails to advance in the secretory pathway due to recognition as a misfolded protein by the endoplasmic reticulum (ER) quality control machinery and consequent targeting for proteasomal degradation. Overexpression of NPC1^{I1061T} led to late endosomal localization of the mutant protein and functional complementation of the *NPC* mutant phenotype, likely as a result of a small proportion of NPC1^{I1061T} mutant protein that folded correctly and was thus able to escape ER quality control. Our findings provide support for use of chemical chaperones as approaches to treat NPC disease caused by the *NPC1^{I1061T}* mutation.

MATERIALS AND METHODS

Cell Culture and Chemicals—Normal human skin fibroblasts were obtained from ATCC (20). The human homozygous *NPC1^{I1061T}* mutant human fibroblast cell lines (NIH 83.16, NIH 89.79, NIH 90.39, and NIH 95.47) were generously provided by Daniel Kraft and David Marks (Mayo) (15). M12 cells are mutant CHO-K1 cells that contain a deletion of the *npc1* locus (8). To generate *npc1*-null cells expressing WT NPC1, NPC1^{I1061T}, and NPC1^{P692S}, M12 cells were infected with retrovirus prepared by transient transfection of 293GPG packaging cells with the ΔU3m*npc1*-WT-GFP, ΔU3m*npc1-I1061T*-GFP, and ΔU3m*npc1-P692S*-GFP constructs, respectively, as previously described (3). Mouse embryonic fibroblasts were isolated from WT C57BL/6 mice. Cells were maintained in monolayer culture at 37 °C with 5% CO_2. All fibroblasts cell lines were passaged in media containing Dulbecco's modified Eagle's medium with 10% (v/v) inactivated fetal bovine serum, 2 mM glutamine, 50 units/ml penicillin, and 50 μg/ml streptomycin. CHO-derived cell lines were maintained in 1:1 Dulbecco's modified Eagle's medium:Ham's F-12 with 5% (v/v) fetal bovine serum, 2 mM glutamine, 50 units/ml penicillin, 50 μg/ml streptomycin. Transfection of M12 cells was performed using Lipofectamine Plus reagent as previously described (3). Transient transfections of *NPC1^{I1061T}* fibroblasts were performed using a primary cell line nucleofector kit and apparatus from Amaxa (20). Dulbecco's modified Eagle's medium, fetal bovine serum, glutamine, Ham's F-12 medium, Lipofectamine Plus, and penicillin/streptomycin were obtained from Invitrogen. Paraformaldehyde was obtained from EM Sciences. All restriction enzymes and endoglycosidases were obtained from New England Biolabs. [^{35}S]Cys/Met (11.0 mCi/ml-EasyTag Express Labeling Kit), Western Lightning Chemiluminescent Reagent, and En^{3}Hance were obtained from PerkinElmer Life Sciences. Complete Protease Inhibitor Mixture Tablets, phenylmethylsulfonyl fluoride, and Protein A-agarose were obtained from Roche Applied Science. The β-actin antibody, dialyzed fetal bovine serum, filipin, and glycerol were from Sigma. 4-Phenylbutyrate (sodium salt) was from EMD Biosciences. The NPC1 antibody used for immunoprecipitation and Western blotting was a rabbit anti-human NPC1 (raised against residues 1261–1278) (8). The p63 antibody was kindly provided by Jack Rohrer (21).

Plasmids—The ΔU3m*npc1-I1061T*-GFP construct was generated using the QuikChange XL Site-directed Mutagenesis Kit (Stratagene), using the ΔU3m*npc1*-WT-GFP construct as a template (3). ΔU3m*npc1-I1061T* was generated by deletion of the COOH-terminal GFP tag. The presence of the *npc1^{I1061T}* mutation and the entire m*npc1* coding sequence in the expression construct was confirmed by ABI Prism automated sequencing.

Quantification of Human NPC1 Gene Expression—Total RNA was isolated from cells using TRIzol reagent (Invitrogen), and reverse transcribed to cDNA using SuperScriptII RNase H$^-$ reverse transcriptase and random hexamer primers (Invitrogen). cDNA was then amplified for 40 PCR cycles using SYBR Green PCR master mixture (Applied Biosystems) and template-specific primers (50 nM) in an ABI Prism 7500 sequence detector. Primer sequences were as follows: human *NPC1* (forward, 5′-cagctggacaactatacccgaat-3′; reverse, 5′-tggcttcacccagtcgaaat-3′) and human glyceraldehyde-3-phosphate dehydrogenase (forward, 5′-cgagatcccctccaaaatcaa-3′; reverse, 5′-catgcgtccttccacgataccaa-3′). Relative quantification of gene expression was performed using the comparative threshold (C_T) method as described by the manufacturer. Changes in mRNA expression level were calculated following normalization to glyceraldehyde-3-phosphate dehydrogenase expression.

Protein Preparation and Western Blot Analysis—Detergent lysates were prepared by washing cell monolayers three times with phosphate-buffered saline. Cells were then scraped in 500 μl of TNEN$^+$ (50 mM Tris, pH 8.0, 0.15 M NaCl, 2 mM EDTA, 0.5% Nonidet P-40, 1× Complete Protease Inhibitor Mixture, 1 mM phenylmethylsulfonyl fluoride) and incubated on ice for 10 min. Cell lysates were collected into microcentrifuge tubes and nuclei were pelleted by centrifugation at 1000 × *g* for 10 minutes at 4 °C. Supernatants were transferred to new tubes. Proteins in TNEN$^+$ lysates were quantified using the bicinchoninic acid protein assay kit (Pierce). Isolation of microsomes from CHO cell lines was performed as described previously (22). Non-boiled samples were resolved by SDS-PAGE under reducing conditions. Proteins were transferred onto polyvinylidene difluoride (0.45 mm; Millipore) using a semi-dry electroblotter (Owl Scientific). Western blot analysis of NPC1 expression was performed using an affinity purified rabbit anti-human NPC1 at a dilution of 1:2000 and a peroxidase-conjugated donkey anti-rabbit IgG (Jackson Immunoresearch) at 1:5000. Analysis of β-actin expression was performed using a rabbit anti-human β-actin at 1:500 and a peroxidase-conjugated donkey anti-rabbit IgG at 1:5000. Analysis of p63 expression was performed using a rabbit anti-human p63 at 1:5000 and a peroxidase-conjugated donkey anti-rabbit IgG at 1:5000. Detection was performed by chemiluminescence using Western Lightning reagents. Densitometry was performed using Quantity One software (Bio-Rad). For each of the non-peptide competition lanes, both the blot background and the region on the gel between 160 and 220 kDa in the peptide competition lanes (*i.e.* background bands), including the band denoted by the *filled arrow*, were subtracted from total NPC1 immunoreactivity.

Metabolic Labeling and Immunoprecipitation of NPC1 Protein—Pulse-chase labeling of NPC1 protein was achieved following a 1-h treatment in starvation media (Cys/Met-depleted) followed by a 1-h treatment in starvation media supplemented with [^{35}S]Cys/Met (EasyTag Express Labeling Kit). After labeling, total cell lysate was collected in 500 μl of TNEN$^+$

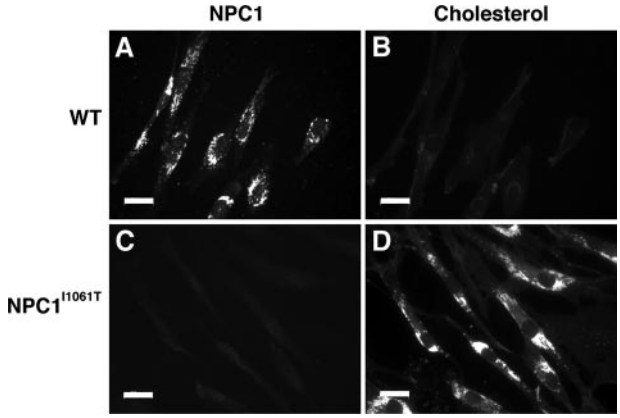

FIGURE 1. **Immunofluorescence staining for NPC1 (*A* and *C*) and filipin staining for cholesterol (*B* and *D*) in WT (*A* and *B*) and *NPC1^{I1061T}* mutant fibroblasts (*C* and *D*).** *Bar*, 50 μM.

buffer (0.5% Nonidet P-40). The lysate was spun at 1000 × *g* for 10 min at 4 °C, the supernatant was collected, pre-cleared with Protein A-agarose, and incubated with NPC1 affinity purified antibody overnight at 4 °C. Protein-antibody complex was pulled down using Protein A-agarose at 4 °C for 45 min. Protein-antibody complex was removed from the Protein A-agarose using 1× Laemmli buffer (Bio-Rad) for 10 min at 37 °C followed by vortexing. For endoglycosidase treatments, immunoprecipitations (IPs) were treated overnight at 37 °C with either Endoglycosidase H (Endo H) or peptide:*N*-glycosidase F in the commercially supplied buffers. Protein was separated by 6% SDS-PAGE and analyzed by autoradiography.

Immunofluorescence Microscopy—Following transfection, cells were plated on 22-mm glass coverslips in 35-mm wells. Cells were cultured 24–72 h, and fixed with 4% paraformaldehyde in phosphate-buffered saline for 30 min. Immunocytochemistry for NPC1 and unesterified cholesterol (filipin staining) was performed as described (5). The coverslips were washed three times with phosphate-buffered saline, mounted (SlowFade, Molecular Probes), and examined by fluorescence microscopy on a Zeiss Axiovert epifluorescence microscope. The following filter sets (Chroma) were used: for filipin, excitation filter 360/40 nm, emission filter 460/50; for GFP, excitation filter 500/20, emission filter 535/30.

LDL-stimulated Cholesterol Esterification Assay—Cholesterol esterification assays were performed as described previously (3).

Statistics—All results are expressed as mean ± S.E. The statistical significance of differences in mean values was determined by single factor analysis of variance. Data shown are representative of at least three similar experiments and are presented as mean ± S.E.

RESULTS

NPC1^{I1061T} Mutant Protein Is Mislocalized and Expressed at Reduced Levels in Human Fibroblasts—In WT human fibroblasts NPC1 protein predominantly distributes to a multivesicular late endosomal compartment (5, 6) (Fig. 1). This contrasts with human fibroblasts homozygous for the *NPC1^{I1061T}* missense mutation, in which NPC1 immunostaining is reduced and the mutant protein fails to localize to late endosomes. The resulting lysosomal free cholesterol accumulation in the *NPC1^{I1061T}* fibroblasts is the hallmark of the *NPC* mutant phenotype (12). Whereas *NPC1* mRNA transcript levels are elevated 1.4–2.4-fold in *NPC1^{I1061T} versus* WT fibroblasts (Fig. 2*A*), NPC1 protein levels are reduced by 85% in the *NPC1^{I1061T}* fibroblasts (Fig. 2, *B* and *C*). Thus, the *NPC1^{I1061T}* substitution affects steady-state levels of endogenously expressed NPC1 protein, possibly by impairing translation of the NPC1 protein or by rendering the protein unstable.

NPC1^{I1061T} Missense Mutation Promotes Rapid Proteasomal Degradation of NPC1 Protein—To assess the effect of the *NPC1^{I1061T}* mutation on stability of the NPC1 protein, we monitored the degradation of the protein in metabolic pulse-chase experiments over a 72-h period. WT and *NPC1^{I1061T}* homozygous fibroblasts were labeled, and NPC1 protein immunoprecipitated and analyzed by autoradiography (Fig. 3, *A* and *B*). Two distinct rates for WT NPC1 protein degradation were observed. From 0–8 h post pulse labeling, WT NPC1 protein exhibited a $t_{1/2}$ of 9 h, whereas from 8 to 72 h, the $t_{1/2}$ was extended to 42 h (Fig. 3*C*). By contrast, NPC1^{I1061T} was degraded with a $t_{1/2}$ of 6.5 h, similar to that of the initial rate of degradation of WT protein (Fig. 3*C*). The maximal level of labeled NPC1 protein was comparable between WT and NPC1^{I1061T} proteins, indicating similar rates in initiation of translation. An important difference, however, between WT and NPC1^{I1061T} protein was the failure of NPC1^{I1061T} to mature to higher molecular weight species (see *open arrow*, Fig. 3*B*).

NPC1^{I1061T} Protein Is Sensitive to Endoglycosidase H—The maturation of the NPC1 protein in the secretory pathway was examined in metabolic pulse-chase experiments in which the sensitivity of the labeled protein to digestion by Endo H was determined. Endo H removes immature high-mannose *N*-linked glycans from proteins. Sensitivity to Endo H digestion indicates that the protein has not advanced beyond the ER in the secretory pathway. Conversely, resistance to Endo H digestion indicates that the glycan residues have been trimmed and/or further modified in the Golgi. Peptide:*N*-glycosidase F removes all *N*-linked glycan residues regardless of the glycan modification. In WT fibroblasts, the steady reduction in the level of Endo H-sensitive NPC1 protein (120-kDa band) is accompanied by a concomitant accumulation of Endo H-resistant NPC1 protein (180-kDa band) (Fig. 4*A*). By contrast, the NPC1^{I1061T} mutant protein is present almost exclusively in the Endo H-sensitive form (Fig. 4*B*). As shown by the peptide competition controls, immunoreactivity detected at 180 kDa in the NPC1^{I1061T} mutant blot is due to nonspecific banding, rather than accumulation of Endo H-resistant NPC1 protein. The more rapid loss of the Endo H-sensitive WT NPC1 species likely reflects the dynamic between degradation of ER-associated NPC1 protein and procession of the immature NPC1 within the secretory pathway (*i.e.* trafficking from ER to Golgi) to generate mature glycoprotein. The apparent molecular weight shift in NPC1 protein in the glycosidase experiments (Fig. 4 *versus* Fig. 3) is an artifact of the glycosidase treatment and buffer system used in the studies. Taken together, the metabolic labeling experiments demonstrate that ~50% of WT NPC1 protein, and nearly all of the NPC1^{I1061T} mutant protein, is ER-retained and targeted for degradation.

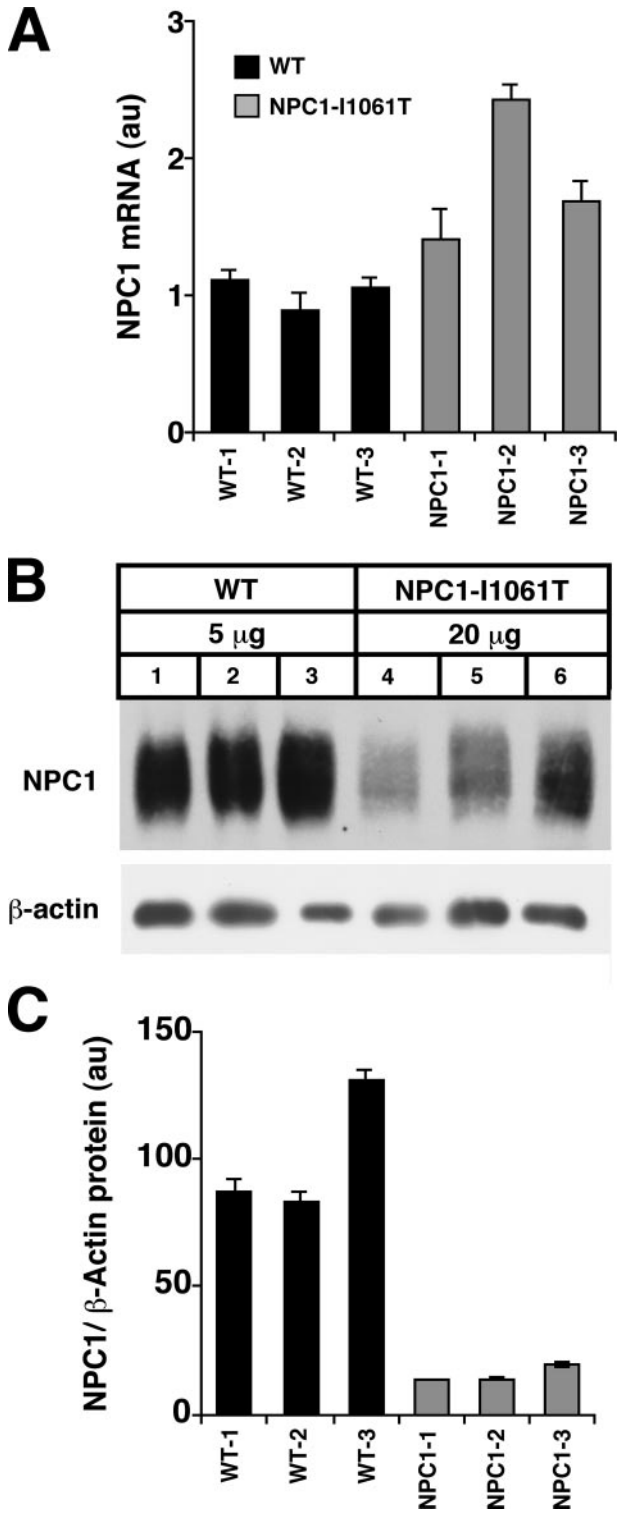

FIGURE 2. **Characterization of NPC1 expression in human fibroblasts homozygous for *NPC1^{I1061T}* mutations.** Data shown are for three independent WT and three independent *NPC1^{I1061T}* human fibroblast cell lines. *A*, real-time quantitative PCR for *NPC1* mRNA levels in WT (*black bars*) and *NPC1^{I1061T}* mutant fibroblasts (*gray bars*). *NPC1* mRNA expression is normalized to glyceraldehyde-3-phosphate dehydrogenase mRNA. *, $p = 0.056$ for mean WT *versus* mean *NPC1^{I1061T}*. *B*, Western blot analysis for NPC1 protein expression in WT and *NPC1^{I1061T}* mutant fibroblasts. Note 4-fold greater loading of protein in *NPC1^{I1061T}* lanes compared with WT lanes. NPC1 expression is normalized to β-actin expression (5 μg/lane). *C*, quantification of NPC1 protein expression in WT (*black bars*) and *NPC1^{I1061T}* mutant fibroblasts (*gray bars*). *, $p < 0.01$ for mean WT *versus* mean *NPC1^{I1061T}*.

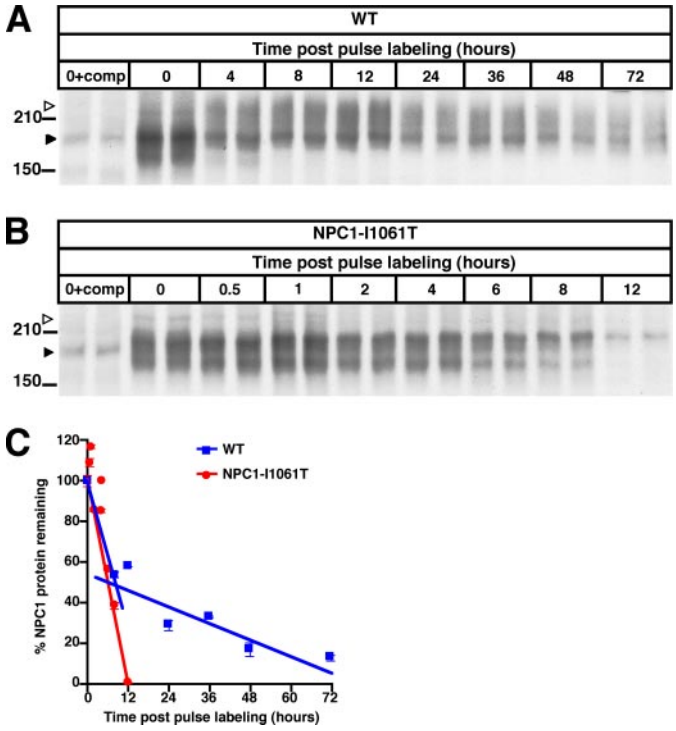

FIGURE 3. **Regulation of NPC1^{I1061T} protein expression by ER quality control.** *A* and *B*, metabolic labeling of newly synthesized NPC1 protein. WT (*A*) and *NPC1^{I1061T}* mutant (*B*) fibroblasts were pulsed for 1 h with [^{35}S]Cys/Met containing media followed by 0–72 h (WT) or 0–12 h (*NPC1^{I1061T}*) chase and IP with NPC1 antibody. For each time point two independent samples are shown. *Left lanes* (*0+comp*) show IP in the presence of excess immunizing peptide (competition). *Closed arrows* identify nonspecific band. Note the shift to higher molecular weight species (*open arrows*) in WT cells from 0 to 4 h, which is absent in the *NPC1^{I1061T}* mutant. *C*, the graph plots densitometric values for radiolabeled NPC1 *versus* time. From 0 to 8 h both WT (*blue line*) and *NPC1^{I1061T}* fibroblasts (*red line*) show similar initial rapid rates of NPC1 protein degradation (WT $t_{1/2} = 9$ h, NPC1^{I1061T} $t_{1/2} = 6.5$ h), whereas from 8 to 72 h WT (*blue line*) NPC1 protein degradation is decreased to $t_{1/2} = 42$ h.

NPC1^{I1061T} Protein Is Selected for ERAD—The ER quality control pathway selects for degradation misfolded and unassembled proteins in the ER (23). To examine whether the NPC1^{I1061T} mutant protein is a substrate for ERAD, we subjected *NPC1^{I1061T}* mutant fibroblasts to treatment with either glycerol or 4-phenylbutyric acid (PBA), chemical chaperones known to stabilize misfolded proteins (24–26). Glycerol and PBA treatments resulted in 1.4- and 1.5-fold increases, respectively, in the level of the mutant protein (Fig. 5, *A* and *B*). Similarly, growth of *NPC1^{I1061T}* mutant fibroblasts at the permissive temperature of 26 °C, which partially rescues the ER processing block of cystic fibrosis transmembrane conductance regulator (*CFTR*) Δ*508* mutant (24, 27), increased NPC1^{I1061T} protein levels 1.7-fold. The stabilizing effects of the chemical chaperones and growth at permissive temperatures on NPC1^{I1061T} provide compelling evidence that the mutant protein is selected for ERAD due to protein misfolding. To determine the metabolic fate of the mutant protein selected for ERAD, *NPC1^{I1061T}* mutant fibroblasts were treated with MG132, a proteasome inhibitor, or chloroquine, a weak base that inhibits lysosomal proteolysis. In the presence of MG132, mutant protein levels were increased 3.5-fold, implicating the proteasomal pathway in degradation of the mutant protein (Fig. 5*C*). By contrast, NPC1^{I1061T} protein levels were reduced 85%

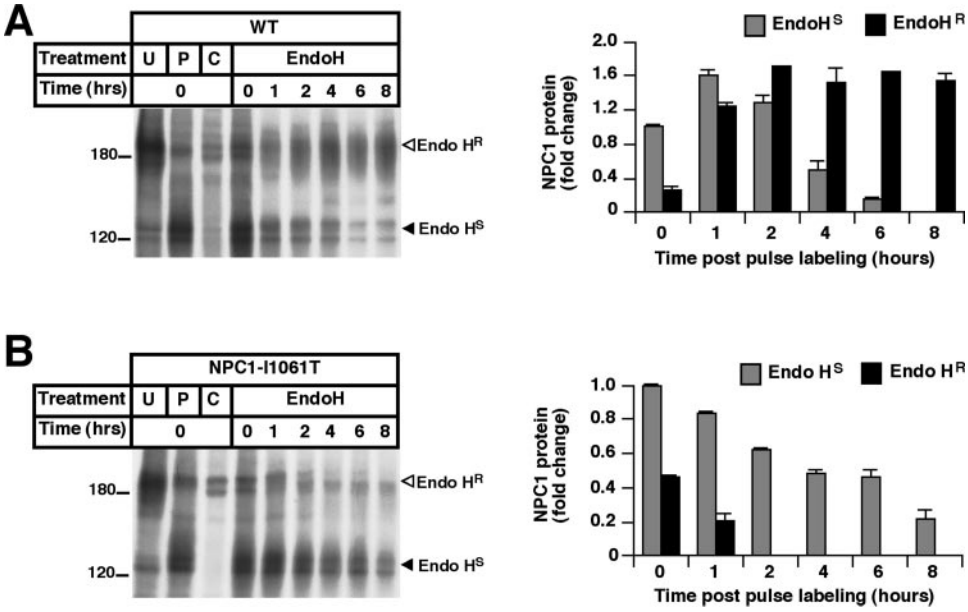

FIGURE 4. **Metabolic labeling of newly synthesized NPC1 protein followed by Endo H treatment.** *A*, WT and *NPC1^{I1061T}* mutant, and *B*, fibroblasts were pulse-labeled as above, followed by 0–8 h chase, IP with NPC1 antibody, and Endo H treatment. *U*, untreated, *P*, peptide:*N*-glycosidase F treated, and *C*, IP in the presence of excess immunizing peptide. *Closed arrows* and *open arrows* indicate Endo H-sensitive and Endo H-resistant species, respectively. Graphs show densitometric values for Endo H-sensitive (*gray bars*) and Endo H-resistant species (*black bars*) in WT (*upper right panel*) and *NPC1^{I1061T}* mutant fibroblasts (*lower right panel*).

after treatment with chloroquine, clearly demonstrating that the mutant protein is not lysosomally degraded.

Overexpression of the NPC1^{I1061T} Protein Rescues the NPC Mutant Phenotype—Previous studies have shown that overexpression of mutant proteins that are misfolded may allow for transit of a small proportion of the mutant proteins through the Golgi (28). Heterologous overexpression of CFTR Δ508 led to escape of mutant protein from ERAD and appropriate localization at the plasma membrane (29, 30). Therefore, we investigated whether overexpression of NPC1^{I1061T} could lead to escape of NPC1^{I1061T} molecules from ERAD and proper targeting to the late endosomal compartment. In transient transfection experiments, we found that overexpression of GFP-tagged NPC1^{I1061T} in *npc1*-deficient CHO cells led to appropriate late endosomal localization of the mutant protein, and to clearance of lysosomal free cholesterol (Fig. 6*A*, *top panels*). By contrast, overexpression of the non-functional GFP-tagged NPC1^{P692S} in *npc1*-deficient CHO cells failed to mobilize lysosomal free cholesterol (Fig. 6*A*, *bottom panels*) (3). This finding indicated that forced overexpression of an NPC1 mutant was not sufficient to complement the cholesterol accumulation phenotype. We likewise found that heterologous expression of NPC1^{I1061T} could rescue the mutant phenotype in human *NPC1^{I1061T}* mutant fibroblasts (Fig. 6*B*). To quantify the function of the NPC1^{I1061T} mutant, we transiently expressed either WT NPC1 or NPC1^{I1061T} GFP fusion proteins in the *npc1*-deficient CHO cells and monitored for clearance of unesterified lysosomal cholesterol by filipin staining (31). We found that the mutant protein was nearly as effective as WT protein in mobilizing lysosomal cholesterol, although at each time point examined the complementation efficiency of the *npc1^{I1061T}* mutant was slightly less than that of WT (Fig. 7, *A*–*C*). To exclude the possibility that the NPC1^{I1061T} mutant protein might have been artificially stabilized by the COOH-terminal GFP fusion, we compared the ability of the NPC1^{I1061T} mutant expression constructs, with and without the GFP tag, to complement *npc1*-deficient CHO cells. At 72 h post-transfection, we found that expression of the *npc1^{I1061T}* construct achieved 90.5% complementation, whereas expression of the *npc1^{I1061T}*-GFP construct achieved 87.2% complementation (Fig. 7*D*). Thus, the functionality and/or stability of the GFP-tagged NPC1^{I1061T} protein cannot be attributed to the presence of the GFP tag.

As an independent approach to confirm the function of the NPC1^{I1061T} mutant protein, we monitored the egress of LDL-derived cholesterol from the lysosomes using an LDL cholesterol esterification assay. For these experiments, we isolated *npc1*-deficient CHO cells stably re-expressing WT NPC1, NPC1^{I1061T}, or NPC1^{P692S}. In comparison to primary mouse embryonic fibroblasts, NPC1 protein was overexpressed ~2-fold in the WT *NPC1*, *NPC1^{I1061T}*, and *NPC1^{P692S}* cell lines (Fig. 8, *A* and *B*). (Because the rabbit polyclonal antibody does not efficiently recognize hamster NPC1 protein, mouse embryonic fibroblasts rather than CHO cells were used to assess relative NPC1 expression.) We found that overexpression of NPC1^{I1061T} corrected the biochemical defect to 53% of WT CHO cells (Fig. 8*C*). Overexpression of the NPC1^{P692S} mutant protein, which appropriately localizes to late endosomes but is non-functional (3), failed to stimulate cholesterol esterification. Taken together, the complementation and esterification assay data demonstrate that if the NPC1^{I1061T} mutant protein can escape ER quality control, it is properly localized to late endosomes and is functional with respect to mobilization of endosomal cholesterol.

DISCUSSION

Protein misfolding has been implicated in the pathogenesis of over 30 human diseases, including cystic fibrosis, α_1-antitrypsin deficiency, and lysosomal storage diseases (32, 33). In these disorders, mutant proteins that fail to achieve proper conformation are targeted for ERAD, resulting in loss of function and disease. In the present study, we demonstrate that the *NPC1^{I1061T}* missense mutation, the most prevalent NPC disease allele, disrupts NPC1 protein trafficking by promoting ER-mediated degradation of the mutant protein. Overexpression of the NPC1^{I1061T} mutant unexpectedly led to appropriate late endosomal localization of the mutant protein and correction of the mutant phenotype. We conclude that the NPC1^{I1061T} mutant protein is functional with respect to cholesterol trafficking, but is unstable because it is misfolded and targeted by

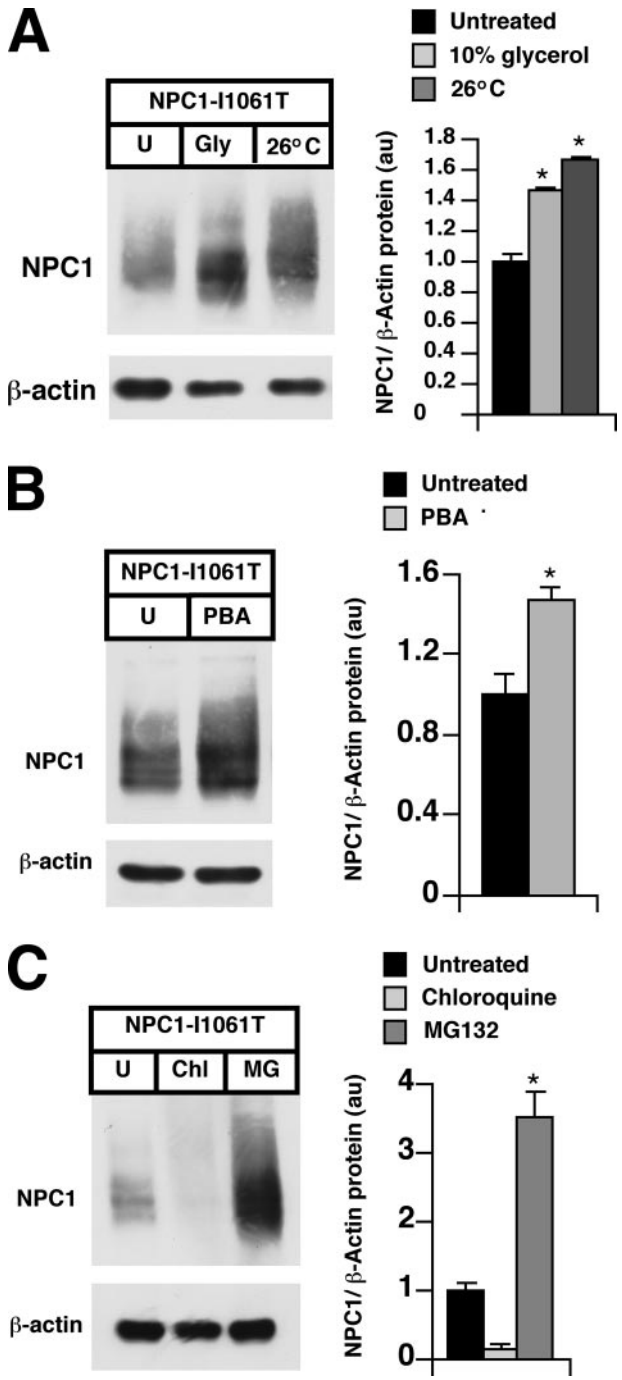

FIGURE 5. **NPC1^{I1061T} protein is proteasomally degraded.** *A*, *NPC1^{I1061T}* cells were treated for 24 h in 10% glycerol or incubated at 26 °C, and cell lysates were subjected to Western blot analysis for NPC1 expression. A representative blot is shown and the graph displays NPC1 expression normalized to β-actin. *, $p < 0.05$ for 26 °C *versus* untreated, $p = 0.057$ for glycerol *versus* untreated. *B*, *NPC1^{I1061T}* cells were treated for 24 h with 20 μM PBA, and lysates were subjected to Western blot analysis for NPC1 expression. A representative blot is shown and the graph displays NPC1 expression normalized to β-actin. *, $p < 0.05$ for PBA *versus* untreated. *C*, *NPC1^{I1061T}* cells were treated for 24 h with the proteasome inhibitor MG132 (50 μM) or with the lysosome inhibitor chloroquine (10 μM), and lysates were subjected to Western blot analysis for NPC1 expression. A representative blot is shown and the graph displays NPC1 expression normalized to β-actin. *, $p < 0.05$ for MG132 *versus* untreated.

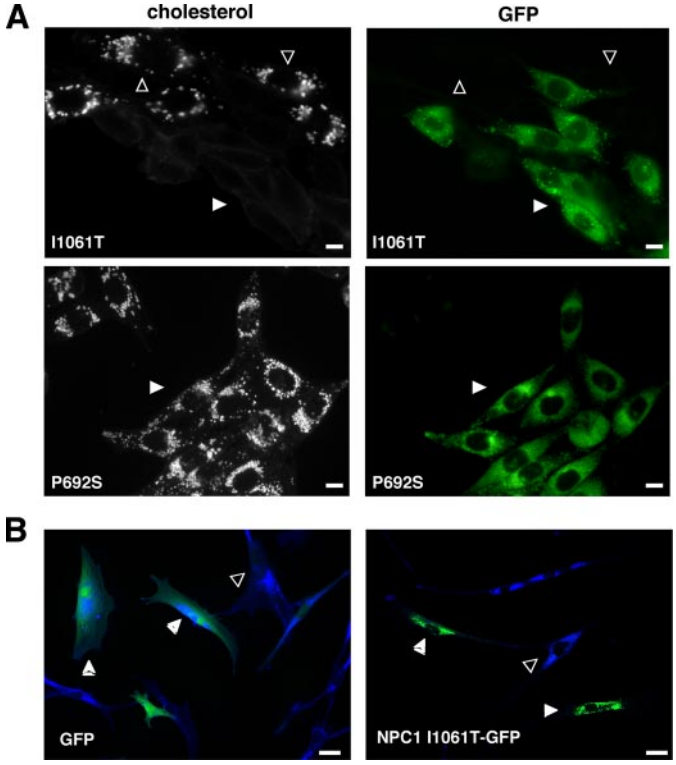

FIGURE 6. **Overexpression of NPC1^{I1061T} rescues the cholesterol accumulation phenotype in *npc1*-null cells.** *A*, *npc1*-deficient CHO cells were transiently transfected with either *npc1^{I1061T}*-GFP (*top panels*) or *npc1^{P692S}*-GFP (*bottom panels*) constructs and stained with filipin for unesterified cholesterol. Cells were examined by immunofluorescence for cholesterol (*left panels*) and GFP expression (*right panels*). *npc1*-null cells expressing *npc1^{I1061T}*-GFP (*top panels*, *closed arrows*) are filipin-negative, whereas non-transfected cells (*top panels*, *open arrows*) are filipin-positive indicative of *NPC1* mutant phenotype. *npc1*-null cells expressing the non-functional mutant *npc1^{P692S}bottom panels*, *closed arrows*) remain filipin-positive. *Bar*, 10 μM. *B*, *NPC1*-deficient human fibroblasts were transiently transfected with either GFP (*left panel*) or *npc1^{I1061T}*-GFP (*right panel*) constructs and tested for the ability to complement the *NPC1* phenotype. Merged immunofluorescence images are shown for GFP (*green*) and cholesterol (*blue*) staining. In the *right panel*, *npc1*-null cells expressing *npc1^{I1061T}*-GFP (*closed arrows*) are complemented (low cholesterol staining), whereas in the *left panel* GFP expressing cells (*closed arrows*) are not complemented (high cholesterol staining). Non-transfected cells (*open arrows*) do not exhibit complementation. *Bar*, 50 μM.

the ER quality control machinery for proteasomal degradation. Our study provides the first description of an ER trafficking defect as a mechanism for human NPC disease, and suggests novel approaches for treatment of this progressive neurodegenerative disorder.

The function of ER quality control machinery is to prevent delivery of proteins to sites of function until they are properly folded, thereby limiting cytotoxicity of accumulated misfolded proteins (25, 34). Proteins recognized as misfolded by quality control are degraded through the actions of the ubiquitin-proteasome pathway. ER quality control not only targets mutant proteins, but also wild-type proteins that have been exposed to damaging conditions or that are slow to achieve conformation because they require extensive post-translational modifications (35). Whereas mature WT NPC1 protein that has progressed to post-ER compartments (*i.e.* Endo H-resistant) exhibits a half-life of 42 h, the half-life of ER-associated (*i.e.* Endo H-sensitive) WT NPC1 protein is only 9 h. Our data indicate that nearly half of the newly synthesized WT NPC1 protein is degraded within the ER. Similar ER-mediated degradation of immature species has been reported for other large, polytopic proteins, such as CFTR (36), and is likely due to failure of these heavily glyco-

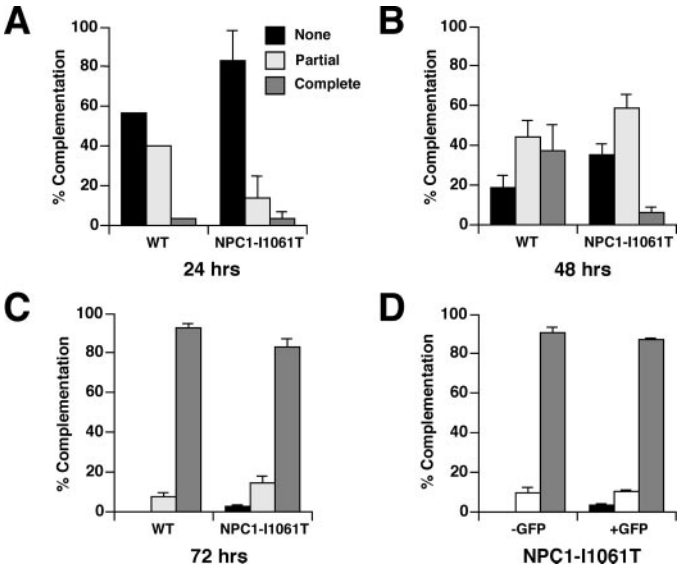

FIGURE 7. **Time course of complementation of *npc1*-null CHO cells by transient expression of WT *npc1*-GFP or *npc1^{I1061T}*-GFP.** *Graphs* show the extent of complementation of *npc1*-null CHO cells by the WT and *npc1^{I1061T}* constructs at 24 (*A*), 48 (*B*), and 72 (*C*) h post-transfection. Transfected cells (GFP-positive) were either scored as none (<20% complementation), partial (20–80% complementation), or complete (>80% complementation). p = NS for WT *npc1*-GFP *versus npc1^{I1061T}*-GFP at 72 h. *D*, comparison of the extent of complementation of *npc1*-null CHO cells by the *npc1^{I1061T}* and *npc1^{I1061T}*-GFP constructs at 72 h post-transfection. p = NS for *npc1^{I1061T} versus npc1^{I1061T}*-GFP.

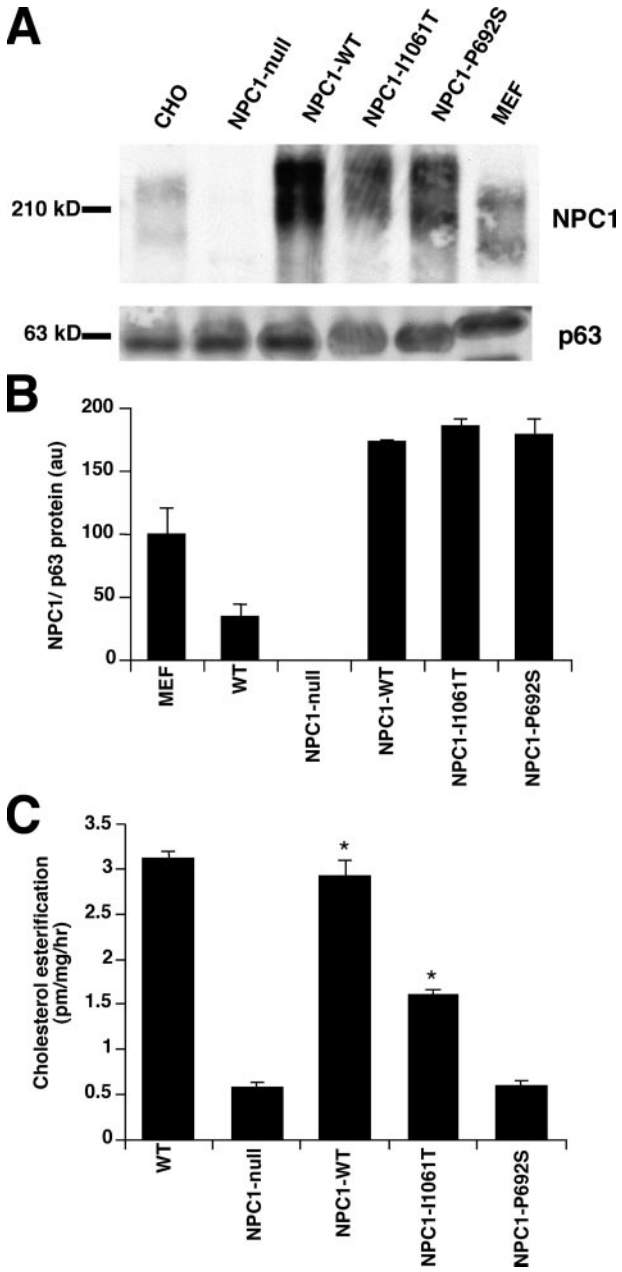

FIGURE 8. **Overexpression of NPC1^{I1061T} rescues the cholesterol esterification defect in *npc1*-null cells.** *A*, Western blot analysis of NPC1 and p63 protein expression in microsomes (5 μg/lane) isolated from WT CHO cells; *npc1*-null CHO cells; *npc1*-null cell lines expressing WT NPC1, NPC1^{I1061T}, and NPC1^{P692S}; and WT mouse embryonic fibroblasts. The lower *M*, for NPC1 protein in WT mouse embryonic fibroblasts likely represents differences in glycosylation patterns between the hamster and murine cell lines. *B*, quantification of NPC1 protein in *npc1*-null cell lines expressing WT NPC1, NPC1^{I1061T}, and NPC1^{P692S}. NPC1 expression is normalized to expression of p63, a resident ER membrane protein, and densitometry presented as mean of duplicate lanes. *C*, LDL-stimulated cholesterol esterification in WT CHO cells; *npc1*-null CHO cells; and *npc1*-null cell lines expressing WT NPC1, NPC1^{I1061T}, and NPC1^{P692S}. Assays were performed in triplicate and values represent mean ± S.E. *, $p < 0.05$ for mean cholesterol esterification in *npc1*-null cells *versus npc1^{I1061T}* cells.

sylated proteins to properly fold prior to arrival at the ER quality control checkpoints.

The presence of the *NPC1^{I1061T}* mutation further accelerates degradation of immature NPC1 protein by the ER quality control machinery. We find that the half-life of ER-associated NPC1^{I1061T} protein is reduced to 6.5 h, and that almost none of the endogenously expressed protein escapes the ER. The *NPC1^{I1061T}* substitution could affect NPC1 protein stability by introducing structural features into the NPC1 protein that cause its recognition as a misfolded protein. The significant increase in NPC1^{I1061T} protein levels in cells grown at permissive temperatures or in cells administered chemical chaperones (*e.g.* glycerol and PBA) provide evidence that the mutant form of the protein is misfolded. Alternatively, newly synthesized NPC1^{I1061T} protein may be slower to achieve conformation, thus prolonging association with ER chaperones and increasing the likelihood of selection for ERAD.

A key finding in our study was the demonstration that overexpression of the NPC1^{I1061T} protein rescues the mutant phenotype in *npc1*-deficient cells. We show that at least a portion of the overexpressed mutant protein was correctly targeted to late endosomes, and importantly, properly functioned in mobilization of free cholesterol from this compartment, as determined by clearance of lysosomal free cholesterol and re-esterification of LDL-derived cholesterol. Overexpression of misfolded proteins leading to ER escape has been shown previously for other proteins, such as the CFTR Δ508 mutant (29). A possible explanation for "leakiness" of the mutant NPC1 protein is that enforced overexpression of the protein saturated the ER quality control machinery (37). Perhaps a more plausible explanation, based on a kinetic model, is that a small proportion of the nascent NPC1^{I1061T} protein is able to fold correctly and therefore escape the quality control checkpoints (38). Assuming a fixed rate for leakiness for the I1061T mutant (*e.g.* 2–5% of the I1061T molecules achieve proper conformation), a sufficient quantity of correctly folded I1061T molecules could escape the

ER as a result of overexpression, leading to complementation of the mutant phenotype. In the present study we demonstrate that a 2-fold overexpression of NPC1^{I1061T} protein is able to partially correct the biochemical phenotype in *npc1*-null cells. Assuming that the level of properly targeted NPC1 protein required for complete complementation of the cholesterol trafficking defect is ~10%, akin to the level of hydrolases required for enzymatic correction of other lysosomal disorders (39), it is reasonable to conclude that in human fibroblasts as much as 2.5–5% of the endogenous NPC1^{I1061T} protein could exit the ER in the proper conformation. Whereas steady-state NPC1 protein levels were increased when the mutant fibroblasts were cultured at permissive temperatures or exposed to chemical chaperones that stabilize protein, the overall effect on efficiency of NPC1^{I1061T} protein folding does not appear to be sufficient to correct the cholesterol trafficking defect (not shown). On the other hand, identification of chemical chaperones that enhance the efficiency of NPC1^{I1061T} protein folding through high throughput small molecule screens has the potential to develop new and effective approaches for the treatment of NPC1 disease. Such an approach might not only benefit subjects with the *NPC1^{I1061T}* genotype, but subjects with other missense mutations, in particular the *G992W* and *P1007A* genotypes that likewise effect the cysteine-rich luminal domain. In future studies these and other NPC1 mutants could be screened to determine whether the mutant proteins are similarly misfolded and respond to treatment with chemical chaperones. If this is indeed the case, there is the potential that a significant percentage of *NPC1* subjects could benefit from small molecule-based chaperone therapy.

Acknowledgment—We are grateful for Stuart Kornfeld for critical review of the manuscript.

REFERENCES

1. Ory, D. S. (2000) *Biochim. Biophys. Acta* **1529,** 331–339
2. Carstea, E. D., Morris, J. A., Coleman, K. G., Loftus, S. K., Zhang, D., Cummings, C., Gu, J., Rosenfeld, M. A., Pavan, W. J., Krizman, D. B., Naqle, J., Polymeropoulos, M. H., Sturley, S. L., Ioannou, Y. A., Higgins, M. E., *et al.* (1997) *Science* **277,** 228–231
3. Millard, E., Gale, S., Dudley, N., Zhang, J., Schaffer, J., and Ory, D. (2005) *J. Biol. Chem.* **280,** 28581–28590
4. Davies, J. P., and Ioannou, Y. A. (2000) *J. Biol. Chem.* **275,** 24367–24374
5. Frolov, A., Srivastava, K., Daphna-Iken, D., Traub, L. M., Schaffer, J. E., and Ory, D. S. (2001) *J. Biol. Chem.* **276,** 46414–46421
6. Neufeld, E. B., Wastney, M., and Patel, S., Suresh, S., Cooney, A. M., Dwyer, N. K., Roff, C. F., Ohno, K., Morris, J. A., Carstea, E. A., Incardona, J. P., Strauss, J. F., III, Vanier, M. T., Patterson, M. C., Brady, R. O., Pentchev, P. G., and Blanchette-Mackie, E. J. (1999) *J. Biol. Chem.* **274,** 9627–9635
7. Zhang, M., Dwyer, N., Neufeld, E. B., Love, D. C., Cooney, A., Comly, M., Patel, S., Watari, H., Strauss, J. F., III, Pentchev, P. G., Hanover, J. A., and Blanchette-Mackie, E. J. (2001) *J. Biol. Chem.* **276,** 3417–3425
8. Millard, E. E., Srivastava, K., Traub, L., Schaffer, J. E., and Ory, D. S. (2000) *J. Biol. Chem.* **275,** 38445–38451
9. Neufeld, E. B., Cooney, A. M., Pitha, J., Dawidowicz, E. A., Dwyer, N. K., Pentchev, P. G., and Blanchette-Mackie, E. J. (1996) *J. Biol. Chem.* **271,** 21604–21613
10. Wojtanik, K. M., and Liscum, L. (2003) *J. Biol. Chem.* **278,** 14850–14856
11. Liscum, L., and Faust, J. R. (1987) *J. Biol. Chem.* **262,** 17002–17008
12. Pentchev, P. G., Comly, M. E., Kruth, H. S., Vanier, M. T., Wenger, D. A., Patel, S., and Brady, R. O. (1985) *Proc. Natl. Acad. Sci.* **82,** 8247–8251
13. Chen, W., Sun, Y., Welch, C., Gorelik, A., Leventhal, A. R., Tabas, I., and Tall, A. R. (2001) *J. Biol. Chem.* **276,** 43564–43569
14. Choi, H. Y., Karten, B., Chan, T., Vance, J. E., Greer, W. L., Heidenreich, R. A., Garver, W. S., and Francis, G. A. (2003) *J. Biol. Chem.* **278,** 32569–32577
15. Park, W. D., O'Brien, J. F., Lundquist, P. A., Kraft, D. L., Vockley, C. W., Karnes, P. S., Patterson, M. C., and Snow, K. (2003) *Hum. Mutat.* **22,** 313–325
16. Scott, C., and Ioannou, Y. A. (2004) *Biochim. Biophys. Acta* **1685,** 8–13
17. Fernandez-Valero, E. M., Ballart, A., Iturriaga, C., Lluch, M., Macias, J., Vanier, M. T., Pineda, M., and Coll, M. J. (2005) *Clin. Genet.* **68,** 245–254
18. Millat, G., Marcais, C., Rafi, M. A., Yamamoto, T., Morris, J. A., Pentchev, P. G., Ohno, K., Wenger, D. A., and Vanier, M. T. (1999) *Am. J. Hum. Genet.* **65,** 1321–1329
19. Watari, H., Blanchette-Mackie, E. J., Dwyer, N. K., Watari, M., Burd, C. G., Patel, S., Pentchev, P. G., and Strauss, J. F., 3rd (2000) *Exp. Cell Res.* **259,** 247–256
20. Frolov, A., Zielinski, S. E., Crowley, J. R., Dudley-Rucker, N., Schaffer, J. E., and Ory, D. S. (2003) *J. Biol. Chem.* **278,** 25517–25525
21. Schweizer, A., Rohrer, J., Slot, J. W., Geuze, H. J., and Kornfeld, S. (1995) *J. Cell Sci.* **108,** 2477–2485
22. Gale, S. E., Frolov, A., Han, X., Bickel, P. E., Cao, L., Bowcock, A., Schaffer, J. E., and Ory, D. S. (2006) *J. Biol. Chem.* **281,** 11082–11089
23. Werner, E. D., Brodsky, J. L., and McCracken, A. A. (1996) *Proc. Natl. Acad. Sci. U. S. A.* **93,** 13797–13801
24. Sato, S., Ward, C. L., Krouse, M. E., Wine, J. J., and Kopito, R. R. (1996) *J. Biol. Chem.* **271,** 635–638
25. Shearer, A. G., and Hampton, R. Y. (2004) *J. Biol. Chem.* **279,** 188–196
26. Rubenstein, R. C., Egan, M. E., and Zeitlin, P. L. (1997) *J. Clin. Investig.* **100,** 2457–2465
27. Denning, G. M., Anderson, M. P., Amara, J. F., Marshall, J., Smith, A. E., and Welsh, M. J. (1992) *Nature* **358,** 761–764
28. Spear, E. D., and Ng, D. T. (2003) *Mol. Biol. Cell* **14,** 2756–2767
29. Dalemans, W., Barbry, P., Champigny, G., Jallat, S., Dott, K., Dreyer, D., Crystal, R. G., Pavirani, A., Lecocq, J. P., and Lazdunski, M. (1991) *Nature* **354,** 526–528
30. Sharma, M., Benharouga, M., Hu, W., and Lukacs, G. L. (2001) *J. Biol. Chem.* **276,** 8942–8950
31. Watari, H., Blanchette-Mackie, E. J., Dwyer, N. K., Watari, M., Neufeld, E. B., Patel, S., Pentchev, P. G., and Strauss, J. F., 3rd (1999) *J. Biol. Chem.* **274,** 21861–21866
32. Aridor, M., and Hannan, L. A. (2000) *Traffic* **1,** 836–851
33. Aridor, M., and Hannan, L. A. (2002) *Traffic* **3,** 781–790
34. Sifers, R. N. (2003) *Science* **299,** 1330–1331
35. Sitia, R., and Braakman, I. (2003) *Nature* **426,** 891–894
36. Ward, C. L., and Kopito, R. R. (1994) *J. Biol. Chem.* **269,** 25710–25718
37. Gelman, M. S., and Kopito, R. R. (2002) *J. Clin. Investig.* **110,** 1591–1597
38. Kopito, R. R. (1999) *Physiol. Rev.* **79,** S167–173
39. Schueler, U. H., Kolter, T., Kaneski, C. R., Zirzow, G. C., Sandhoff, K., and Brady, R. O. (2004) *J. Inherit. Metab. Dis.* **27,** 649–658